17th International Conference on the Application of Computer
Science and Mathematics in Architecture and Civil Engineering
K. Gürlebeck and C. Könke (eds.)
Weimar, Germany, 12–14 July 2006

Hybrid Approach of Wave Number Integration-Boundary Integral Equation Method for Site Effect Estimation of a Laterally Varying Seismic Region

T. Schanz [a], F. Wuttke [a] and P. Dineva [b]

[a] Laboratory of Soil Mechanics, Bauhaus-University, Weimar, Germany,

tom.schanz@bauing.uni-weimar.de

frank.wuttke@bauing.uni-weimar.de

[b] Institute of Mechanics, Bulgarian Academy of Sciences, Sofia, Bulgaria

petia@imbm.bas.bg

Abstract

A new hybrid Wave Number Integration-Boundary Integral Equation Method (WNI-BIEM) is proposed for computation of seismic signal at receiver points of local multilayered geological region situated in inhomogeneous half-space with seismic source in it. The proposed hybrid analytically-numerical technique gives efficient tool for synthesis of theoretical seismograms accounting for the properties of the seismic source, wave path and local region of interest. The validation study of the accuracy of the proposed method is presented by solution of benchmark example. The numerical simulation reveals that the developed hybrid method is able to demonstrate the sensitivity of the obtained synthetic signals on the seismic source properties, on the heterogeneous character of the wave path and on the site effects of the local stratified geological deposit.

KEYWORDS: Seismic wave propagation, Laterally varying seismic region, Hybrid Wave Number Integration-BIE Method, Site effects.

1. INTRODUCTION

The adequate computation of synthetic seismograms is based on the appropriate choice of models describing the seismic source, the wave path and the local region of interest, see Figure 1. Essentially three main groups of approaches threat the problem and they are analytical [1-2], numerical [3-4] and hybrid [5-6]. The analytical methods are restricted to media with simple geometry, with inhomogeneity dimensions that are considerably larger than the prevailing wavelengths, and therefore are only of limited use for zoning studies. In opposite, the numerical technique is suitable for studying complex sedimentary basins but it requires much CPV time and memory. To make use of the advantages of the analytical and numerical approaches, the development of the so-called hybrid technique is recently very actual and of big importance.

In the hybrid computational schemes the numerical methods are applied only in the laterally heterogeneous part of the medium that is a small part of it, whereas the laterally homogeneous part is treated by analytical methods as ray methods and their modifications. To the authors knowledge the used in the literature hybrid computational schemes [7-9] are mainly based on the finite difference and modal summation methods. Although the well known advantages [10] of the Boundary Integral Equation Method (BIEM), discussed below, there is a lack of the hybrid methods used in the wave propagation theory that are based on the BIEM. The facilities of the BIEM in comparison with other numerical techniques are:

- ***Reduction in the dimension of the problem***

It is possible to model the surface of the problem geometry only and as a result substantially to reduce the size of the problem dimensionality plus the size of the resulting system of algebraic equations. The size of the obtained after discretization system of algebraic equations is much smaller then the same one obtained at application of other numerical methods as finite element or finite difference methods and this is a big advantage, although it is non-symmetric and fully-populated.

- ***Semi-analytical character of the method*** as far as it is based on the fundamental solution or Green function of the governing differential equation in the studied problem

- ***High level of accuracy*** is achieved since numerical quadrature techniques are directly applied to the boundary integral equations that are an exact solution to the problem at hand.

- ***Solution at each internal point in the domain is expressed in terms of boundary values without recourse to domain discretization***. This main facility is very important when wave propagation problems are being solved in multilayered geological regions, because only the boundaries between layers are discretisized, not their volumes as it is when finite element or finite difference methods are used.

- ***The fundamental solution used in the construction of the boundary integral equations obeys the radiation*** *condition and thus infinitely extended boundaries are automatically incorporated*, in opposite to other numerical methods where special viscous boundaries have to be used in order to satisfy the Sommerfield radiation conditions at infinite.

This work aims to combine the facilities of both methods the analytical Wave Number Integration Method (WNIM) and the numerical BIEM. The main objective of this study is to develop an accurate and efficient hybrid approach for synthesis of theoretical seismograms in a laterally varying seismic region accounting for the main characteristics of the seismic source, the wave path from the source to the area of interest and the local geological media with complex geometry. The proposed hybrid technique is based on the WNIM for investigating wave propagation in inhomogeneous half-space, while BIE method is used for synthesis of theoretical seismograms on the free surface of the local multilayered, heterogeneous soil region.

2. PROBLEM FORMULATION

Consider finite local geological region $\Omega_{LGR} = \bigcup_{i=1}^{N} \Omega_i$ with N non-parallel layers Ω_i and free surface topography situated in inhomogeneous half-space Ω_0 with a seismic source in it, as it is shown in Figure 1. We consider vertical varying of the mechanical properties in the wave path Ω_0 and it is modeled with series of M homogeneous flat layers Γ_i, parallel to the free surface, overlaying the homogeneous half-space where is the seismic bed, i.e. $\Omega_0 = \bigcup_{k=1}^{M} \Gamma_k$. All soil layers are isotropic, elastic and homogeneous. Let ρ_k, $\alpha_k = \sqrt{\lambda_k + 2\mu_k / \rho_k}$, $\beta_k = \sqrt{\mu_k / \rho_k}$, $k = 1,2,...M$ are the density, body wave velocities α_k, β_k and Lame constants λ_k, μ_k of each $k-th$ layer in the wave path, while the material properties in the $i-th$ layer of the local geological region are: ρ_i, $C_P^i = \sqrt{\lambda_i + 2\mu_i / \rho_i}$, $C_S^i = \sqrt{\mu_i / \rho_i}$, $i = 1,2,...N$. It is considered "in-plane" P-SV wave propagation problem.

The aim is to obtain the synthetic seismograms in some receiver points along the free surface of the local region Ω_{LGR}. The problem posed consists of two sub-problems: (a) first sub-problem concerns wave propagation in inhomogeneous wave path from the seismic source to the outside boundary Λ of the local geological region Ω_{LGR}, see Figure 1. This part is solved by the analytical WNI method and the final product is the displacement field along the boundary Λ between the local region and the half-space; (b) second sub-problem deals with seismic wave propagation in the finite soil strata with non-parallel layering and surface or subsurface relief, using as boundary condition the wave field on the boundary Λ, obtained at solution of the first sub-problem. This part is solved by BIEM.

2.1. Boundary value problem formulation for seismic wave propagation in a vertically inhomogeneous half-space with a buried earthquake source.

The governing equations are Lame-Navier partial differential equations:

$$\left(\alpha^2 - \beta^2\right) u_{j,ji}(x,z,t) + \beta^2 u_{i,jj}(x,z,t) = \ddot{u}_i(x,z,t) \quad \text{in } Q_B = \Omega_B \times (0,T) \tag{1}$$

Where longitudinal and shear wave velocities are different for different layers, T is the duration of the seismic load, u_i is the displacement, $\ddot{u}_i$ is the acceleration.

The next boundary conditions are hold: ***(a)*** Sommerfeld radiation condition in infinite; ***(b)*** The tractions at the free surface have to be zero $p_i(x,z,t)=0$; ***(c)*** the continuity of displacements and tractions at the interface between two layers. The initial conditions for $t=0$ are: $u_i(x,z,0)=u_{i0}(x,z)$; $\dot{u}_i(x,z,0)=\dot{u}_{i0}(x,z)$, where $\dot{u}_i$ is the velocity.

2.2. Boundary value problem formulation for seismic wave propagation in a finite multilayered geological region

The governing equation is (1), where longitudinal C_P and shear C_S wave velocities are different for different layers. The boundary conditions are: ***(a)*** On the free-surface of the local geological region all tractions are zero, i.e. $p_i(x,z,t)=0$; ***(b)*** On the boundary between two soil layers the continuity conditions are satisfied: $u_i(x,z,t)\big|_{\Gamma_{\Omega_i}} = u_i(x,z,t)\big|_{\Gamma_{\Omega_{i+1}}}$ and the motion must be such that all dynamic forces acting onto the interface are in dynamic equilibrium: $p_i(x,z,t)\big|_{\Gamma_{\Omega_i}} = -p_i(x,z,t)\big|_{\Gamma_{\Omega_{i+1}}}$; ***(c)*** On the boundary Λ between the geological column and the half-space it is hold: $u_i(x,z,t)\big|_{\Lambda} = u_i^{free-field}(x,z,t)\big|_{\Lambda}$ for $(x,z)\in\Lambda$, where "free-field" motion means the displacement on Λ in the case there is no local geological region. i.e. displacements obtained as solution of the BVP defined in the section 2.1. The initial conditions for $t=0$ in Ω_B are: $u_i(x,z,0)=u_{i0}(x,z)$; $\dot{u}_i(x,z,0)=\dot{u}_{i0}(x,z)$ where $\dot{u}_i$ is the velocity.

The solution of the boundary-value problem defined in 2.1. and 2.2. is a vector-value function $u_i(x,z,t)\in C^2(Q_B)\bigcap C^1(\overline{Q}_B)$, such that $p_i(x,z,t)\in C^1(Q_B)\bigcap C\ (\overline{Q}_B)$, which satisfy the system (1) and the boundary and initial conditions given above, where $C^k(K)$ is the set of k times continuously differentiable functions in K (see [11]).

3. METHODOLOGY

3.1. Wave Number Integration Method for solution of the sub-problem 2.1.

The basic equations (1) are decoupled by application of the decomposition theorem. The decoupled partially differential equations can be transformed into a system of ordinary differential equations by using the integral transform method regarding the time and space. The obtained solution is the displacement function of the subproblem 2.1 depending on the frequency ω, on the space coordinates (x, z) and the position in depth of the embedded source:

$$\overline{u}^l(x,z,\omega)=\int_{-\infty}^{\infty}\left(E_{11}^l\Lambda_d^l\hat{R}_u^{l-1}+E_{12}^l\Lambda_u^l\right)\hat{T}_u^l\cdot\ldots\cdot\hat{T}_u^{S-1}\left(B^{S+}D^S-B^{S-}\right)^{-1}\Delta Q\exp(i\zeta x)\,d\zeta \qquad (2)$$

with the wave number ζ, the generalized reflection / transmission (R / T) coefficients $\hat{T}_u^k = \left(I - R_d^k \hat{R}_u^{k-1}\right)^{-1} T_u^k$ and $\hat{R}_u^k = R_u^k + T_d^k \hat{R}_u^{k-1} \hat{T}_u^k$ (k=1,…,S- 1) of the layers above the source layer and $\hat{T}_d^k = \left(I - R_u^k \hat{R}_d^{k+1}\right)^{-1} T_d^k$ and $\hat{R}_d^k = R_d^k + T_u^k \hat{R}_d^{k+1} \hat{T}_d^k$ (k = M-1,…,S) for the layers below to the source layer S. Subscript indices *u* and *d* are for negative and positive z-direction or for up coming and down going waves. At the interface between two layers the R/T coefficients for incoming waves from the negative (u-up) are R_u^k and T_u^k and positive (d-down) z-directions are correspondingly R_d^k and T_d^k (k- number of the preceding layer). For the hybrid method we need to determine the displacements on the interface between the finite local region and infinite region. For the particular example depicted in Fig 2 we have to obtain the dynamic displacement vector of the first layer and therefore $l = 1$ is only used in (2). The term Λ_u^k describes the diagonal matrices of the exponential terms in negative (u-up)- and Λ_d^k positive (d-down) z-direction in the k-th layer. The term $\hat{R}_u^{l-1} = \hat{R}_u^0$ is the reflection coefficient at the free surface, that is the upper boundary of the first layer. The layer with the embedded source is splitted in two imaginary layers $S-$ and $S+$. B^{S+}, D^S and B^{S-} are integrated R/T coefficients in this layer. Following the approach given in [12] and [13] the source ΔQ was considered as a stress-discontinuity between the layers $S-$ and $S+$.

To avoid the singularities at the integration path a weak damping in the wave velocities is used. Finally, the displacement function in frequency domain is obtained after integration over all wave numbers along the integration path. By application of inverse Fourier transform regarding the time the displacements in time domain are calculated.

3.2. Boundary Integral Equation Method for solution of the sub-problem 2.2.

In order to exclude the time variable and to solve the initial boundary-value problem defined in section 2.2., Fourier transform is applied to the time variable. The governing partial differential equation is now of elliptic type, which is solved by the displacement based BIEM in the transformed Fourier domain. The governing equations for displacement components in frequency domain need to be solved in conjunction with the transformed boundary conditions for a finite set of discrete values of the transform parameter ω. Once this is done for a sufficient number of values of the transform parameter, a numerical inversion must be performed on the relevant variables to obtain the time-dependent solution.

The BIEM formulation of the BVP yields the usage of the next BIE for every layer Ω_m separately:

$$C_{ij}\bar{u}_j(x,z,\omega) = \int_{\Gamma_{\Omega_m}} U_{ij}^*(x,z,x_0,z_0,\omega)\bar{p}_j(x_0,z_0,\omega)d\Gamma - \int_{\Gamma_{\Omega_m}} P_{ij}^*(x,z,x_0,z_0,\omega)\bar{u}_j(x_0,z_0,\omega)d\Gamma \qquad (3)$$

m=1,2,3…N; $S_B = \Gamma_{\Omega_1} \cup \Gamma_{\Omega_2} \ldots \cup \Gamma_{\Omega_i} \ldots \cup \Gamma_{\Omega_N}$; Here: C_{ij} are constants depending on the geometry at the collocation point (x,z); $(x,z),(x_0,z_0)$ denote the position vectors of the field

and running points respectively; Γ_{Ω_m} is the boundary of the Ω_m layer; $\overline{u}_j$ and $\overline{p}_j$ are unknown displacements and tractions on the boundaries in the Fourier domain; U_{ij}^*, P_{ij}^* are the displacement and traction fundamental solutions in frequency domain [6].

After discretization of the displacement BIE in the Fourier domain by BEM, overcoming of weak and strong singularities in the obtained integrals and satisfaction of the given boundary conditions an algebraic complex system according to the unknown displacement and traction is obtained and solved. The inverse FFT is applied in order to obtain solution in time, i.e. to obtain synthetic seismograms on the free surface of the local geological region.

4. VALIDATION STUDY

The proposed hybrid WNI-BIEM has been tested by solution of a benchmark example that can be solved by both–the pure WNIM and by the proposed new hybrid WNI-BIEM. The geometry of the geological structure model is presented in Figure 2a. The local geological region in Figure 2a is a valley $L_1R_1T_1P_1$ and it is placed in the first layer of a layered half-space. The coordinates of the corner points (in meters) are: $T_1(100,0)$; $P_1(-100,0)$; $L_1(110,270)$; $R_1(-110,270)$. The mechanical properties of the local geological region are the same as ones of the first layer in the layered half-space, i.e. this seismic scenario concerns the solution of the 1D wave propagation problem. In this case it is possible to solve the problem for seismic wave propagation by both methods - by the pure WNIM and by the proposed here new hybrid WNI-BIEM. The comparison between studied WNI-BIEM solutions against pure WNIM results can evaluate and place the accuracy bounds of the developed hybrid computational technique.

The thickness, the density ρ_i, the longitudinal wave velocity α_i, the shear wave velocity β_i and the depth of the layers presenting a continuously non-homogeneous half-space are given in Table 1. It is considered two wave paths-wave path 1 and wave path 2 with different mechanical properties. For the first calculations of the new hybrid WNI-BIEM a buried vertical line source were defined in the depth of -2 km in the case of wave path 1 and in the depth of -6 km in the case of wave path 2 (table 1). The source term was assumed as a Ricker wavelet of the second order.

Figure 3a-h show that frequency dependent displacement components at receiver point (0, 0) for both wave paths obtained by the WNIM and by the hybrid WNI-BIEM are almost identical. This fact demonstrates that the proposed hybrid method works accurately. This validation study is necessary to be done for each new soil local region and new seismic scenario, because the comparison between the pure analytical method and the proposed hybrid method allows establishing control over the accuracy of the BIEM part of calculations that depends on the correct mesh discretization. The accuracy condition at BIEM discretization procedure demands that $\lambda/l_{BE} \geq 10$, where l_{BE} is the length of the boundary element, λ is the length of the seismic signal. So, it is clear that the high accuracy results demand the finer BEM mesh for waves with higher frequencies and for softer soil layers, where the wave length is shorter.

5. NUMERICAL EXAMPLE

In order to illustrate the efficiency of the proposed hybrid method it is analyzed the response of a multilayered valley with irregular interfaces and the free surface relief, see Figure 2b. The finite local soil stratum has three layers with non-parallel interfaces and there is a free-surface relief in the form of a semi-circle canyon with radius $r = a = 30m$. The coordinates of the points indicating the geometrical boundaries of the layers are:

$T_0(30,0)$; $T_3(60,0)$; $T_2(90,0)$; $T_1 100,0)$; $P_0(-30,0)$; $P_3(-60,0)$; $P_2(-90,0)$; $P_1(-100,0)$; $L_1(110,270)$; $R_1(-110,270)$; $L_2(90,180)$; $R_2(-90,180)$; $L_3(60,90)$; $R_3(-60,90)$.

The mechanical properties of the geological region are given in Table 2 and the properties of the wave path are those of wave path 2, see Table 1. The seismic source characteristics are the same as those described in section 4.

Numerical results that demonstrate the possibility of the presented here hybrid WNI-BIE method to illustrate the site effects of a laterally varying seismic region are shown in Figure 4-7. Displacement amplitudes at receiver point $(80,0)$ are depicted versus frequency in Figure 4. Two curves are shown for two different seismic scenarios: (a) inhomogeneous half-space modeled by horizontal and parallel layers with properties of the wave path 2 and this geometry concerns the solution of the 1D wave propagation problem; (b) inhomogeneous half-space consisting of horizontal and parallel layers with mechanical characteristics equal to those of the wave path 2 plus multilayered valley, see Figure 2b. The analogous results are presented in Figure 5 but for the receiver point $T_1(30,0)$ that is the edge of the canyon. Figures 4-5 clearly show both: (a) the site effects, i.e. the dynamic response in the two receiver points on the free surface are different; (b) the importance to account for the specific geometrical properties of the laterally varying seismic area-1D solution is not adequate to the reality when the geological region is multilayered and with topographic peculiarities. The difference between 1D and 2D solutions is not so great for the point $(80,0)$ which is relatively away from the canyon, while for the edge of the canyon, i.e. point $T_1(30,0)$ this difference is quite greater. Amplitude –frequency characteristics of the seismic signal are presented in Figure 6 for a line of four receivers: $(100,0)$; $(60,0)$; $(30,0)$; $(15.,26.)$ on the free surface of the local multilayered valley. It can be seen again the clearly shown site effects in the seismic wave field-the signal for the two displacement components decrease along the direction from point T_1 to point T_0, however in the points inside the canyon there is increasing of the seismic signal, due to the complex diffraction wave field influenced by the layers and the relief edges. These results clearly display the great significance of locally generated surface waves at the valley's edges. Figure 7 and 8 shows the obtained synthetic seismograms at the same receiver points. The same effects of amplification and deamplification of the seismic signal due to the laterally varying area can be seen.

While simple and intuitively appealing, the proposed hybrid approach may suffer of some drawbacks and particular care is required from the analyst. Strong impedance contrasts and the response at higher frequencies are among the issues that require special attention. The obtained numerical results account for the properties of all components that influence on the seismic signal-the earthquake source, the wave path and the multilayered geological zone. Each one of these parts has its strong and important influence on the seismic wave before its entering in the engineering structure.

6. CONCLUSION

The new hybrid Wave Number Integration-Boundary Integral Equation Method is proposed. The analytically-numerical approach combines WNIM and BIEM. Each of the two techniques is applied in that part of the geological model where it works most efficiently. The BIEM is used in the local stratified geological area while WNIM is applied for simulation the wave propagation from the source position to the local region of interest.

The main advantage of this hybrid tool, in comparison with other computational methods, is that it can taking into consideration seismic source, wave path and local soil effects. This allows to be calculated the local wavefield from a seismic event, both for small (a few kilometers) and large (a few hundreds of kilometer) epicenter distances. The path from the source position to the local region is approximated by a geological structure composed of a sequence of flat homogeneous layers. The simulation of a realistic incident wave field obtained by WNIM is used as input in the BIEM computations. The BIEM permits the modeling of complex multilayered structures with surface and subsurface topography in the final part of the propagation path.

The validation study of the accuracy of the proposed method is presented by solution of benchmark example.

The obtained by the WNI-BIE method seismic signal is adequate to the earth surrounding and it can be used as a necessary base at solution of the next important geotechnical and civil engineering problems: (*) seismic wave propagation with accounting for the more complex mechanical behavior of the soil as poroelasticity, anisotropy, nonelasticity, nonhomogeneity, etc.;(**) soil-structure interaction and its effects on the dynamics of structures during earthquake; (***) solution of inverse problems for dynamic site characterization and identifying the soil profiles.

Acknowledgment: *The authors acknowledge the support of the NATO Science for peace program under the grant number CLG982064.*

REFERENCES

1. Wuttke, F. (2005) Site characterization using surface waves, PhD-thesis (German), Bauhaus-University Weimar

2. Wuttke, F., Schmidt, H.-G., Schanz, T. Geotechnical site investigation of surface waves considering higher modes, Proc. 13th World Conf. on Earthquake engineering, Vancouver, 2004.

3. Wolf, J. and Song, C. (1996) *Finite-element modeling of unbounded media,* Wiley and Sons.

4. Dineva P, Gavrilova E. (2000) Waves propagation in a multi-layered geological region. Part II: Transient case, *International Journal of Seismology and Earthquake Engineering,* IIEFS, Teheran, I.R. Iran, Vol.2, No.4, 1-8.

5. Panza, G.F., Romanelli, F., Vaccari, Fr. (2000) Seismic wave propagation in laterally heterogeneous anelastic media: theory and applications to seismic zonation, *Advances in Geophysics,* Vol. 43, 1-95.

6. Dineva, P., Vaccari, F., Panza, G. (2003) Hybrid Modal summation-BIE method for site effect estimation of a seismic region in a laterally varying media, to appear in *J. of Theoretical and Applied Mechanics, Bulgarian Academy of Science,* Volume 33(4), 55-88

7. Fah, D., Suhadolc, P., Panza, G.F. (1993) Variability of seismic ground motion in complex media: The Fruili area (Italy). *In: Geophysical exploration in areas of complex geology, II (R. Cassinis, K. Helbig, G.F. Panza, Eds.) Journal of Applied Geophysics,* 30, 131-148.

8. Fah, D., Iodice, C., Suhadolc, P., Panza, G.F. (1993) A new method for realistic estimation of seismic groung motion in megacities: The case of Roma, *Earthquake Spectra,* 9, 643-668.

9. Panza, G.F., Romanelli, F., Vaccai, Fr. (2000) Seismic wave propagation in laterally heterogeneous anelatic media: theory and applications to seismic zonation, *Advances in Geophysics,* Vol.43, 1-95.

10. Beskos, D. (1993) Wave propagation through ground. *In: Boundary Element Techniques in Geomechanics, Eds. G.D. Manolis and T.G. Davies, Computational Mechanics Publications, Southampton and Elsevier, Applied Science, London,* 359-406.

11. Achenbach, J.D. (1973) *Wave propagation in elastic solids,* Elsevier Science Publ. B.V.

12. Hisada, Y. (1994) An efficient method for computing Green's functions for layered half space without sources and receivers at close depth, *BSSA*, 84(5), 1456-1472

13. Harkrider, D.G.(1964) Surface waves in multilayered elastic media; Rayleigh and Love waves from buried sources in multilayered elastic half-space, *BSSA*, 54, 627-679

Table 1. The properties of the layered half-space: wave path 1/wave path 2

Number of soil layer	Thickness (km)	Depth (km)	Density $\rho_i(kg/m^3)$	Wave shear velocity β_i (m/s)	Wave longitudinal velocity α_i (m/s)
1	5.0/0.05	5.0/0.05	2750/2000	3500/1400	6100/2400
2	8.0/0.30	13.0/0.35	2900/2100	3600/1400	6200/2400
3	4.0/0.65	17.0/1.0	3200/2200	4100/1400	7200/2400
4	2.0/1.50	19.0/2.50	3200/2300	4200/1400	7500/2400
5	2.0/1.0	21.0/3.50	3200/2400	4200/1400	7650/2400
6	2.0/1.50	23.0/5.0	3200/2500	4300/2200	7800/3800
7	5.0/2.0	28.0/7.0	3300/2600	4350/2550	8000/4500
8	22.0/5.0	50.0/12.	2900/2650	3800/3100	6800/5400
9	50.0/13.	100.0/25.	3350/2750	4600/3500	8200/6200
10	-/10.	-/35.	-/2900	-/4200	-/7500
11	-/65.	-/100.	-/3350	-/4600	-/8200

Table 2. The properties of the local geological region in Fig.2b

Number of soil layer	Density $\rho(kg/m^3)$	Lame Coefficient $\lambda(N/m^2)$	Shear module $\mu(N/m^2)$	Poisson constant ν	Wave shear velocity β_i (m/s)	Wave longitudinal velocity α_i (m/s)
3	1800	$12.967\ 10^8$	$0.648.\ 10^9$	0.3334	600	1200
2	2000	$1.779\ .10^9$	$2.00\ .10^9$	0.3540	1000	1700
1	2000	$2.709\ .10^9$	$26.45\ .10^8$	0.2530	1150	2000
∞	2000	$1.90\ .10^9$	$3.92\ .10^9$	0.2426	1400	2400

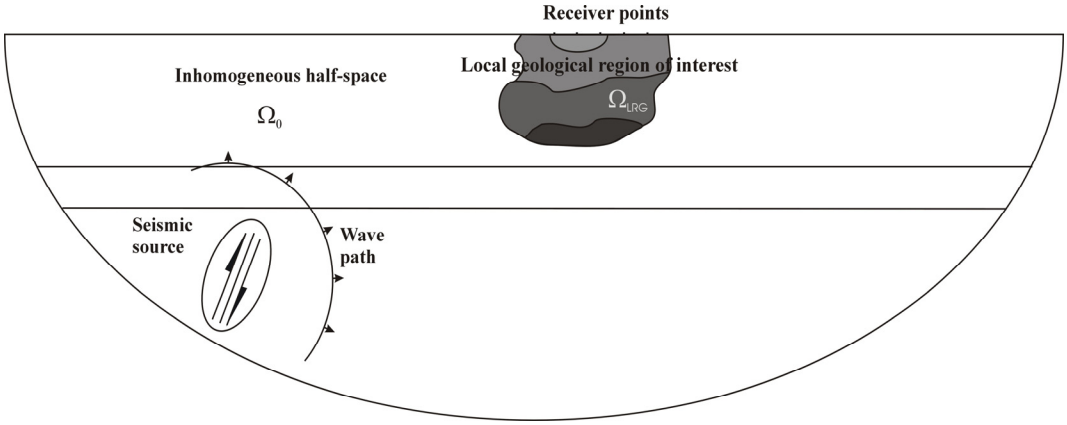

Figure 1: The geometry of the problem

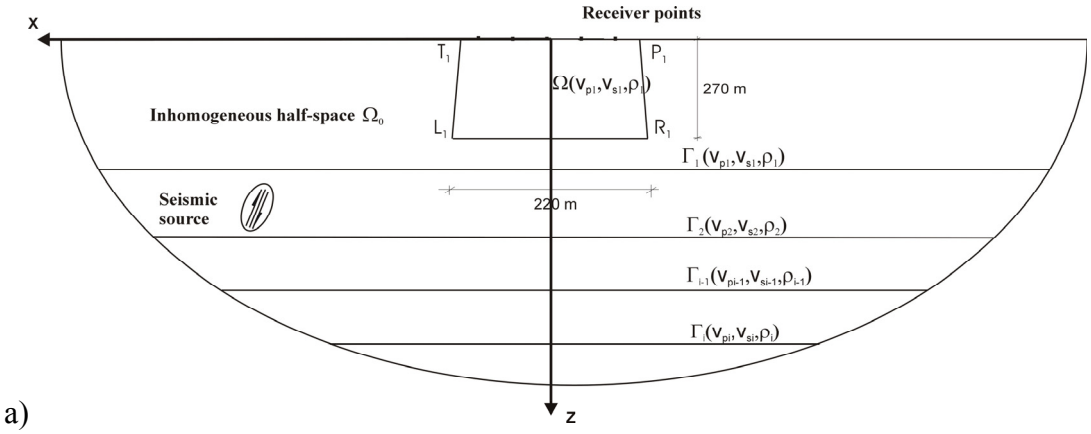

a)

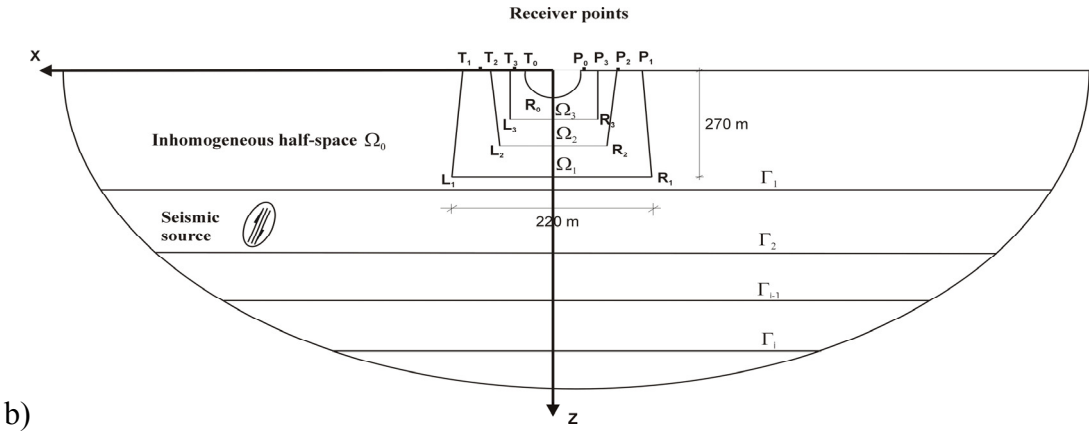

b)

Figure 2a, b: The geometry of the gelogical region

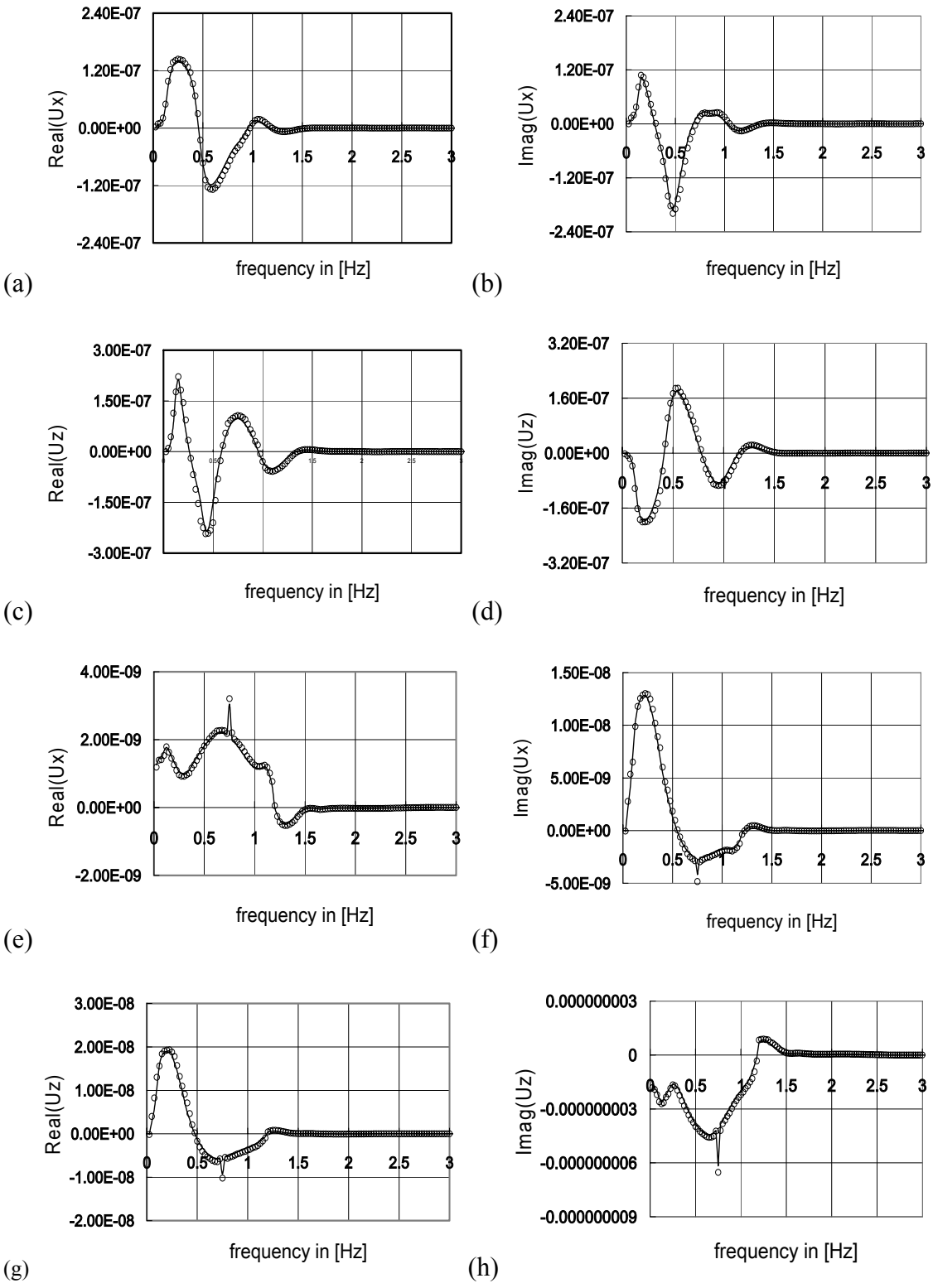

Figure 3: Displacement components at receiver point (0.0); (a)-(d): wave path 2; (e)-(h): wave path 1; — analytical solution; °°°°°° BIEM solution

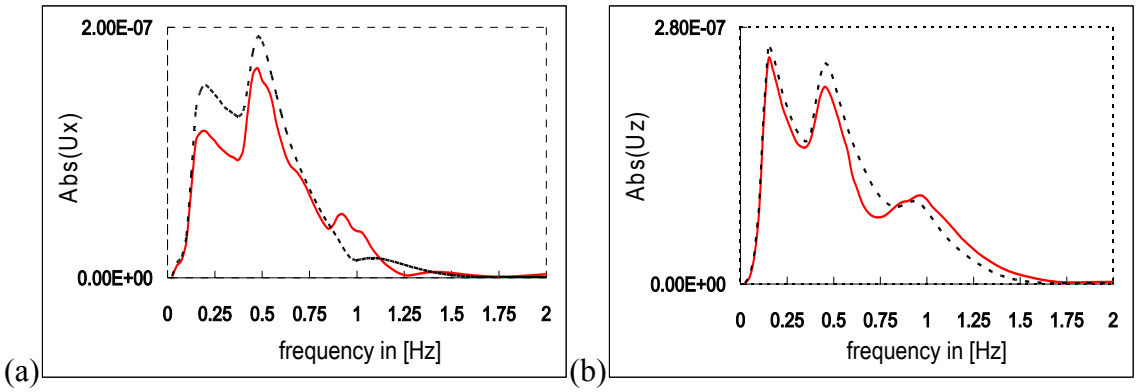

Figure 4: Displacement amplitudes at receiver point $(80, 0)$ in the case: (a) inhomogeneous half-space modeled with horizontal parallel layers (1D solution) -----; (b) inhomogeneous half-space modeled with horizontal parallel layers plus multilayered valley(2D solution) _____;

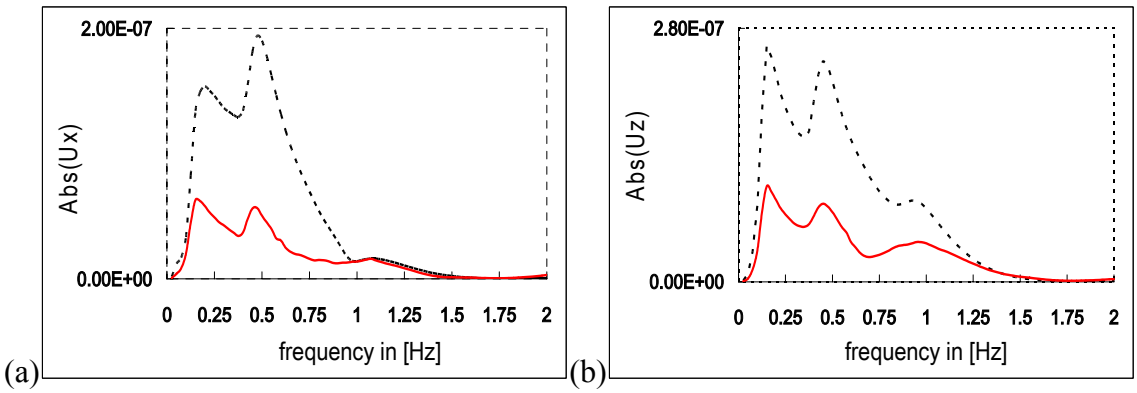

Figure 5: Displacement amplitudes at receiver point $(30, 0)$ in the case: (a) inhomogeneous half-space modeled with horizontal parallel layers (1D solution) -----; (b) inhomogeneous half-space modeled with horizontal parallel layers plus multilayered valley(2D solution) _____;

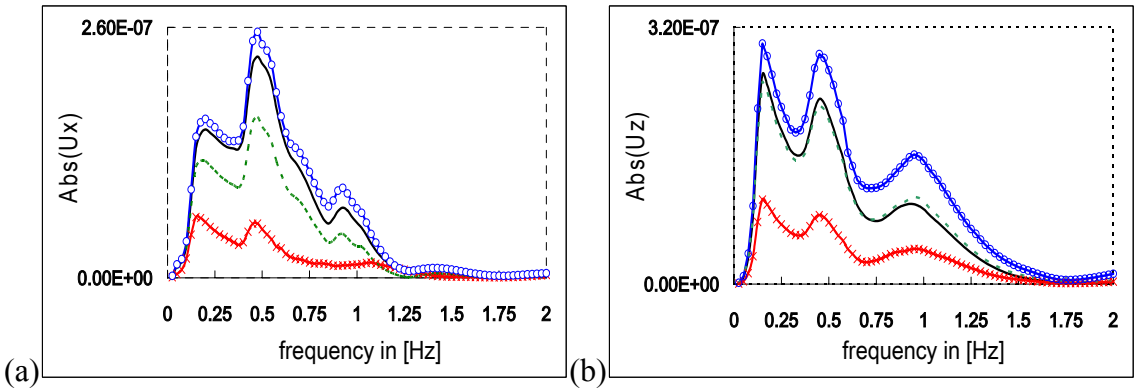

Figure 6: Displacement amplitudes at receiver's points $(100, 0)$ _____; $(60, 0)$ -----; $(30, 0)$ ×××××; $(15., 26.)$ °°°°°° on the free surface of the multilayered valley in Figure 2b.

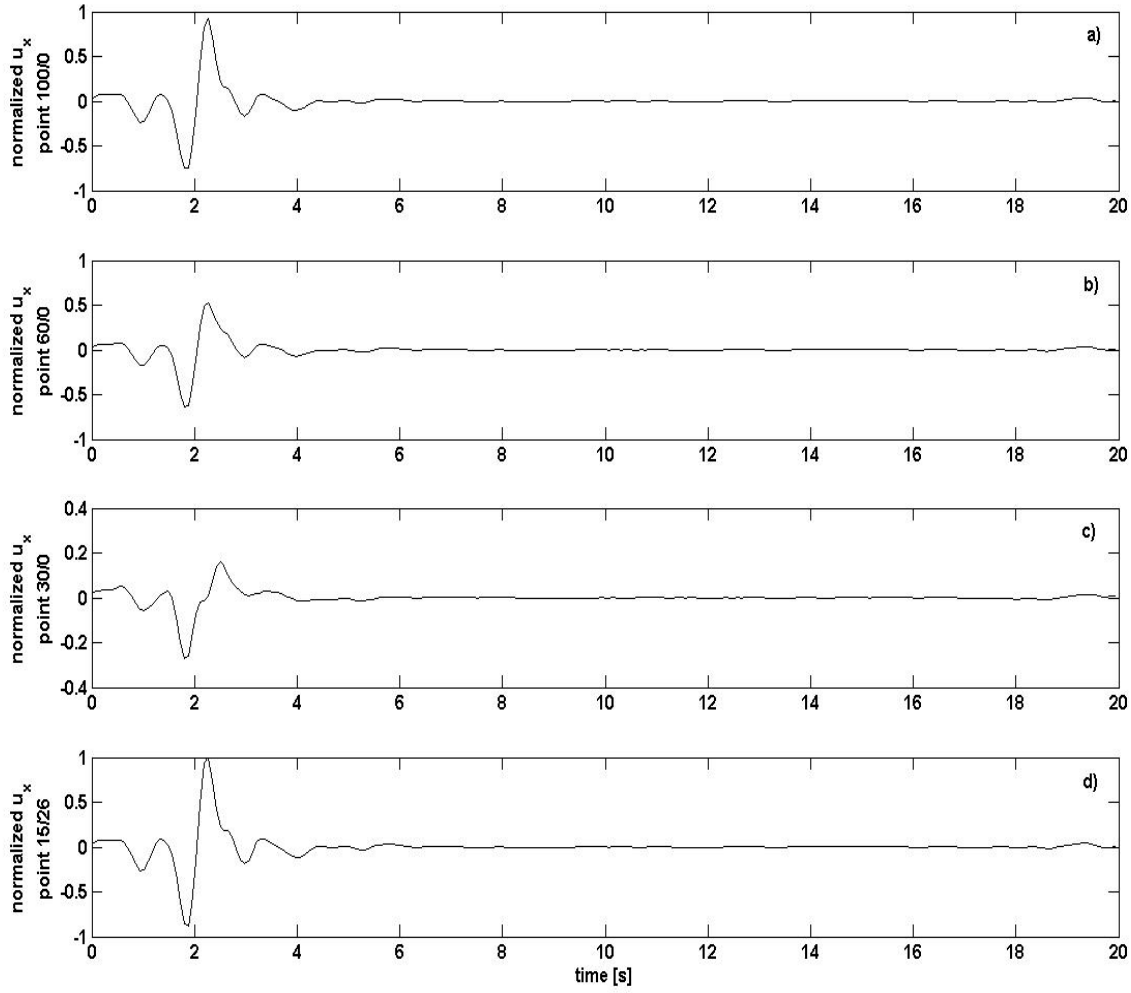

Figure 7: Horizontal displacement u_x versus time t on the free surface of the multilayered valley for the next receiver points: (a) point (15, 26); (b) point (30,0); (c) point (60,0); (d) point (100,0). The seismograms are normalized regarding to point 15/26.

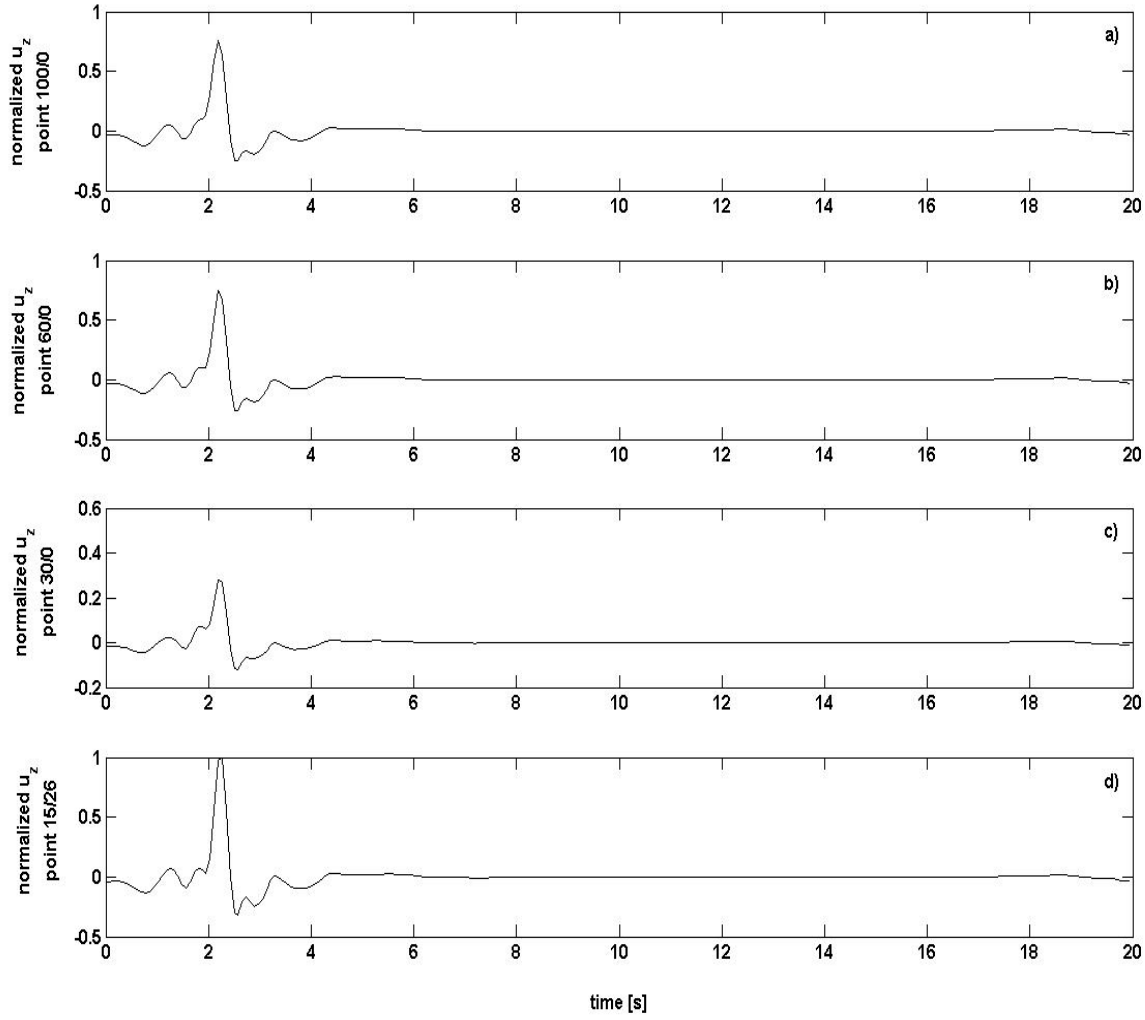

Figure 8: Vertical displacement u_z versus time t on the free surface of the multilayered valley for the next receiver points: (a) point (15, 26); (b) point (30,0); (c) point (60,0); (d) point (100,0). The seismograms are normalized regarding to point 15/26.